Utilization of interferometric light microscopy for the rapid analysis of virus abundance in a river

Céline Roose-Amsaleg, Yasmina Fedala, Catherine Vénien-Bryan, Josette Garnier, Albert-Claude Boccara, Martine Boccara

For publication

Utilization of interferometric light microscopy for rapid analysis of virus abundance in a river

Céline Roose-Amsaleg[a*], Yasmina Fedala[b,c], Catherine Vénien-Bryan[d], Josette Garnier[a], Albert-Claude Boccara[c], Martine Boccara[b,e]

[a]*UMR 7619 METIS, Sorbonne Universités, CNRS, Univ Paris 06, EPHE, 4 place Jussieu, 75005 Paris, France. Tel.: +33 144276256, fax: +33 144274588*

[b]*Institut de Biologie de l'Ecole Normale Supérieure (IBENS), Ecole Normale Supérieure, PSL Research University, CNRS UMR 8197, INSERM U1024, 46 rue d'Ulm, F-75005 Paris, France*

[c]*Institut Langevin, ESPCI ParisTech, PSL Research University, CNRS UMR 7587, 1 rue Jussieu, 75005 Paris, France*

[d]*Institut de Minéralogie, de Physique des Matériaux et de Cosmochimie UMR 7590, Sorbonne Universités, Univ Paris 06, CNRS, MNHN, IRD, 4 place Jussieu, 75005 Paris, France*

[e]*Atelier de Bioinformatique, UMR 7205 ISYEB Sorbonne Universités, Univ Paris 06, CNRS, MNHN, EPHE, 45 rue Buffon, 75005 Paris, France*

*Correspondence and reprints.

E-mail addresses:
celine.amsaleg@upmc.fr (C. Roose-Amsaleg)*
yasmina.fedala@gmail.com
boccara.martine@gmail.com
Catherine.Venien@impmc.upmc.fr
josette.garnier@upmc.fr
claude.boccara@espci.fr

Abstract

There is a constant need for direct counting of biotic nanoparticles such as viruses to unravel river functioning. We used, for the first time in freshwater, a new method based on interferometry differentiating viruses from other particles such as membrane vesicles. In the French Marne River, viruses represented between 42 and 72% of the particles. A spring monitoring in 2014 revealed their increase ($2.1\ 10^{7}$-$2.1\ 10^{8}$ mL^{-1}) linked to an increase in algal biomass and diversity of bacterial plankton. Predicted virus size distributions were in agreement with transmission electron microscopy analysis suggesting a dominance of large viruses (≥60 nm).

Keywords: Virus; Membrane vesicle; Interferometric light microscopy; River

1. Introduction

Water from the Marne River, one of the major tributaries of the Seine River, is used for the production of drinking water for most of the inhabitants of Paris and surroundings. The Marne River used to be subjected to high levels of nutrients (nitrogen and phosphorus), originating from intensive agriculture and urban impact which entailed uneven and recurrent development of algae. These algal blooms were mostly due to diatoms, and secondarily to Chlorophyceae, cyanobacteria forming only low populations in lotic systems [1-3]. Since the 2000s, with the EU Water Framework Directive (2000/60/CE), phosphorus has been considerably reduced [4, 5]. Algal blooms have become scarce, except in dry years. These blooms are mainly observed in spring, when the dilution rate by the discharge becomes lower than algal growth rate. These algal blooms constitute a significant inconvenience for the production of drinking water as, in addition to clogging filters, they increase the water pH [2]. Algal dynamics have been extensively studied for 25 years in order to improve their growing prediction by modeling [6], without explicitly considering the ecological effect of viruses.

In any aquatic environment, viruses, about ten times more abundant than bacteria, control the algal and microbial diversity by lysis and may influence biogeochemical cycles. The abundance of aquatic viruses fluctuates over time, especially with the seasons. A peak of concentration is usually observed during spring-summer periods in surface waters; conversely, a significant decline occurs in autumn-winter [7]. The most common aquatic viruses of phytoplankton are double-stranded DNA-tailed viruses (Caudovirales) such as the following families: Myovirus (head size: 60-145 nm), Podovirus (60-70 nm) and Siphovirus (40-80 nm) which infect prokaryotes while PhycoDNA viruses (large DNA viruses, 100-220 nm) or picorna-like viruses (RNA viruses, 35nm) infect eukaryotic algae [7].

Viral direct counts in any environments remain a critical step requiring a reliable and accurate method [8]. Transmission electron microscopy (TEM) is one of the best techniques

since it allows virus morphotypes to be counted and characterized [9], but is highly time-consuming. Optical methods based on epifluorescence microscopy to detect double-stranded DNA binding fluorophores such as DAPI or SYBR are used extensively. However, these methods are adapted neither for detection of single-stranded DNA, nor RNA viruses [10]. Flow cytometry is also frequently used to enumerate viruses in natural viral assemblages [11]. Most previous methods need expensive equipment and do not distinguish viruses from extracellular membrane vesicles. Extracellular membrane vesicles are another type of aquatic environmental nanoparticle. Produced by organisms from the three domains of life, they are made of lipids and proteins and sometimes contain genetic material, and could thus be mistaken for viruses [12].

We used a new method suitable for all genetic material of viruses and able to differentiate viruses from membrane vesicles. The interferometric light microscope (ILM) combines two measurements for a single nanoparticle (30 to 100nm): its scattered signal and its Brownian motion. The scattered signal is a function of the size and refractive index (related to density) of the particle, while the Brownian motion is a function only of the size of the particle [13]. ILM was utilized to distinguish virus from other particles and then tested to explore the variations of viral communities in the Marne River in spring 2014, expected to be the algal bloom period. The discharge averaging 180 $m^3 s^{-1}$ in January-March decreased to 60 $m^3 s^{-1}$ during the studied period (April-May). The diversity of eukaryotic and bacterial communities was determined simultaneously.

2. Material and methods

2.1. Sample preparation

Water was collected at Saint Maurice (5 km upstream from Paris, 48°48'58.16" North, 002°25'27.35" East), the outlet of the Marne River, at three dates in 2014: April 1st and 22nd and May 14th. Samples were kept in an ice cooler during transport and filtered as soon as they arrived at the laboratory. Two liters of water were first filtered through 0.22 µm filters (PolyVinyliDene Fluoride, Millipore) to collect eukaryotic and prokaryotic plankton. The filters were replaced every 0.5 L to avoid clogging. Filtrates (nanometric fraction) were then concentrated (10,000x) using a 30 KDa cut off filter (Amicon, Millipore).

2.2. Virioplankton characterization and interferometric data processing

We analyzed 5 µL of each filtrate (diluted in PBS to be 50x-concentrated) to collect a stack of 200 images (CMOS camera). The particles were first localized on each image and the average number per frame determined (volume = 10^{-8} mL, concentration in particles of the sample). The maximum scattering intensity of each particle and its trajectory was computed [13]. With these data, we calculated the diameter of each particle from its scattering signal ($diameter_{\_scat}$) and from its Brownian diffusion ($diameter_{\_BM}$). Viral particles are the particles for which the two diameter measurements are close (refractive index n = 1.5). The nanoparticle populations were resolved using the Mclust package of R software with default parameters. Particles for which the $diameter_{\_BM}$ was over 20% larger than the $diameter_{\_scat}$ were considered as empty capsids or vesicles.

2.3.Transmission electron microscopy

Samples (10 µl, 10,000x-concentrated filtrates using Amicon 30 KDa cut off filters) were applied to electron microscope hydrophilic grids coated with carbon film. The specimen was then negatively stained with 2% uranyl acetate. The preparations were examined using a

Jeol 2100 electron microscope equipped with an LaB6 filament, with an acceleration voltage of 200 kV and a 2K x 2K Gatan CCD camera. The nominal magnification was 12.5K. Taking into account the position of the camera, this gives a final magnification at the specimen level of 17.8K. Therefore, the pixel size was 0.8 nm. The pictures (>20) were analyzed to count and sort viruses. Viral capsid diameters were measured using ImageJ software (US National Institutes of Health, Bethesda, MD, USA; [14]).

2.4. Algal biomass

Chlorophyll-a concentrations (*Chl-a*) used as a proxy of the biomass of all photosynthetic organisms were determined by spectrophotometry according to [15].

3. Results and discussion

3.1. Virus-like particle direct counting from river water

Using interferometric light microscopy, we counted particles in water samples previously filtered (<0.2 μm) and concentrated (50x). We observed a sixfold increase in the total number of particles between the beginning (5 10^7 mL^{-1}, April 1st) and the end of the sampling (3 10^8 mL^{-1}, May 14th). We then analyzed the samples from a more qualitative point of view, calculating and plotting for each particle $diameter_{\_scat}$ and $diameter_{\_BM.}$ (Fig. 1). Indeed, any particle differing from a virus showed a similar movement, but a lower scattering signal [13]. We observed other dispersed particles that we predicted to be membrane vesicles [12]. Viruses therefore represented between 42% (2.1 10^7 mL^{-1}, April 1st) and 72% (2.1 10^8 mL^{-1}, May 14th) of the particles, in light of the first and last sampling date (Table 1**)**. This analysis revealed that, in the studied river samples, the number of membrane vesicles could represent (by difference) 28-58 % of the detected particles. Estimating the number of membrane vesicles is a novelty which can provide new insight into the dynamics of viruses and their ecological importance.

3.2. Viral population composition

After excluding membrane vesicles from the analysis, viral populations were further characterized according to their size. Throughout the study, we observed two major peaks centered at 45 and 60 nm diameters (Fig. 2). We classified the predicted viruses into two groups (Table 1): medium-size diameters (40-59 nm) and larger diameters (≥60 nm). In addition to a general increase in the abundance of 45 nm viruses, the proportion of ≥60 nm viruses increased over time (from 7, 19% to 42%, for April 1st and 22nd and May14th, respectively). The viral population of ≥60 nm in size would correspond to myocyanophages and PhycoDNAviruses [16]. However, we detected neither small viruses (30 nm range,

known to infect diatoms) nor very large viruses (>100nm, infecting freshwater green algae). In fact, for particles larger than 100 nm, there was no simple proportionality between the scattering signal and the diameter with ILM [13].

3.3. Comparison of interferometric light and transmission electron microscopy

Using TEM, viruses were observed and counted by major family and sized (diameters). Viruses were classified as Myoviruses, Podoviruses, Siphoviruses or PhycoDNAviruses based on their morphology [16] or spherical particles (the last category corresponds to membrane vesicles, untailed viruses and cellular debris). The percentages of Siphoviruses and Podoviruses were stable between samples, while Myoviruses increased gradually (Fig. S2, S3). We were also able to detect Podoviruses and Myoviruses by DNA amplification (see supplementary information), only in the most virus-concentrated sample from May 14th (data not shown). However the lack of reproducible amplification for Siphoviruses or PhycoDNAviruses suggested either that the amount of template was too small for proper amplification or that the degenerated primers were not suitable. Overall, while the proportion of prokaryotic viruses (Myoviruses and Siphoviruses and Podoviruses) increased (from 24 to 34%), that of eukaryotic viruses (PhycoDNAviruses) decreased (from 9 to 5%).

To compare the distribution of virus diameters between the TEM measurements with those obtained with ILM, we divided the samples into two groups: above and below 60 nm in diameter (Table 1). Although TEM is not a quantitative method, we observed the same distribution patterns for the two latter samples. However, we noticed a discrepancy for the first sample with a low viral concentration, suggesting that we need a threshold concentration of particles (of about 10^9 particles mL^{-1} ,corresponding to at least an average number of 10 particles per frame) to reliably analyze samples by ILM.

3.4. Dynamics of photosynthetic populations during spring 2014 at Saint Maurice

We observed a fivefold increase in *Chl-a* content between April 1st (0.27 µg L^{-1}) and May 14th (1.35 µg L^{-1}), suggesting slight algal growth, but not true algal bloom. Indeed, during a spring algal bloom in the Marne River basin, especially composed of diatoms, the *Chl-a* concentration at St Maurice tended to reach 100 µg L^{-1} or more [1]. The last algal bloom was observed in May 2011 and produced 144 µg L^{-1} of total chlorophyll concentration jerri (*Chl-a* and Pheopigments). On May 14, 2014, diatoms were responsible for 67% of the total algal biomass, with Cyanobacteria representing less than 0.1%.

DNA fingerprinting methods such as PCR-DGGE enable diversity investigation from natural microbial communities by studying the pattern of operational taxonomic units (OTUs). Concerning the aquatic eukaryotic communities, we noted a similar number of OTU (i. e. an approximation of the species richness) between the beginning (April 1st, 21±2.8 OTU) and end of sampling (May 14th, 18±0 OTU) (Fig. S1A). However, community composition showed a net modification, as the patterns of May 14th showed a weak similarity percentage (43.2%) with those of the other two dates.

In contrast, the species richness of aquatic bacterial communities (Fig. S1B) increased between early April and mid-May (from 13±0.7 to 24±1.4 OTU). Subsequently, the bacterial composition varied between dates: communities from April 1st and May 14th shared 43.1% of their OUT, whereas those of April 22nd shared 33.2% with the other two dates.

Thus, in the studied station of the Marne River, over the short sampling period, prokaryotic viruses proliferated. This suggests that their hosts (whose the number of OTUs increased) would also be numerically dominant in the microbial community. In contrast, eukaryotic phytoplankton viruses became a minor part of the viral population, while their hosts harbored less richness (cf. OUT numbers).

In conclusion, we have presented an analysis of virus abundance and diversity in a lotic freshwater environment, the Marne River, during a growth phase of phytoplankton. To analyze this viral abundance, we used an optical method based on interferometric light microscopy. This method proved its efficacy even at a low algal level. With this method, we observed an increase in virus particles and membrane vesicles which has not been previously described in freshwater.

New ecological studies on viral dynamics in freshwater are needed to understand how algal and bacterial dynamics are linked to viral communities and to possibly integrate them into existing ecological models.

Acknowledgments

We would like to thank all the persons who helped us with the experiments: Ellie-Arthur Siéwé-Bobda, Marc Bailly-Bechet, Benjamin Mercier, Fanny Hilaire and Hames Mejri. Dr J-M Guigner is acknowledged for electron microscopy analysis.

References

[1] Garnier J, Billen G, Coste M, Seasonal succession of *Diatoms* and *Chlorophyceae* in the drainage network of the Seine River - Observations and modeling. Limnol Oceanogr 1995;40:750-765.

[2] Garnier J, Némery J, Billen G, Thery S, Nutrient dynamics and control of eutrophication in the Marne River system: modelling the role of exchangeable phosphorus. J Hydrol 2005;304:397-412.

[3] Reynolds CS, Phytoplankton periodicity – the interactions of form, function and environmental variability. Freshwater Biol 1984;14:111-142.

[4] Passy P *et al.*, A-model reconstruction of riverine nutrient fluxes and eutrophication in the Belgian Coastal Zone since 1984. J Marine Syst 2013;128:106-122.

[5] Aissa-Grouz N, Garnier J, Billen G, Long trend reduction of phosphorus wastewater loading in the Seine: determination of phosphorus speciation and sorption for modeling algal growth. Environ Sci Pollut R 2016;doi:10.1007/s11356-016-7555-7.

[6] Garnier J, Billen G, Production vs. Respiration in river systems: An indicator of an "ecological status". Sci Total Environ 2007;375:110-124.

[7] Jacquet S, Miki T, Noble R, Peduzzi P, Wilhelm S, Viruses in aquatic ecosystems: important advancements of the last 20 years and prospects for the future in the field of microbial oceanography and limnology. Adv Oceanogr Limnol 2010;1:97-141.

[8] Wommack KE, Nasko DJ, Chopyk J, Sakowski EG, Counts and sequences, observations that continue to change our understanding of viruses in nature. J Microbiol 2015;53:181-192.

[9] Breitbart M, Marine Viruses: Truth or Dare. Ann Rev Mar Sci 2012;4:425-448.

[10] Forterre P, Soler N, Krupovic M, Marguet E, Ackermann HW, Fake virus particles generated by fluorescence microscopy. Trends Microbiol 2013;21:1-5.

[11] Brussaard CPD, Enumeration of bacteriophages using flow cytometry. Methods Mol. Biol. 2009;501:97-111.

[12] Soler N., Krupovic M, Marguet E, Forterre P, Membrane vesicles in natural environments: a major challenge in viral ecology. Isme J 2015;9:793-796.

[13] Boccara M, Fedala Y, Venien-Bryan C, Bailly-Bechet M, Bowler C, Boccara AC, Full-field interferometry for counting and differentiating aquatic biotic nanoparticles: from laboratory to Tara Oceans. Biomed Opt Express 2016;7:3736-3746.

[14] Abramoff MD, Magalhaes PJ, Ram SJ, Image Processing with ImageJ. Biophotonics International 2004;11:36-42.

[15] Lorenzen C J, Determination of Chlorophyll and Pheopigments – Spectrophotometric equations. Limnol Oceanogr 1967;12:343.

[16] King AMQ, Adams. MJ, Carstens. EB, Lefkowitz EJ, Virus Taxonomy: Classification and Nomenclature of Viruses: Ninth Report of the International Committee on Taxonomy of Viruses. Elsevier, 2011.

Legends to figure

Fig. 1.Analysis of particles present at the Saint Maurice station, an outlet of the Marne River.

Plot of the diameters of particles computed with their scattered signals (Diameter_scat) and Brownian motion ($Diameter_{\_BM}$). Lines indicate refractive indexes of the different particles (viruses and vesicles). The colored bar corresponds to the relative number of characterized particles: the different colors correspond to the Matlab histogram plotted in normalized linear scale. The viruses that possess a refractive index of 1.5 are likely close to this line, while the rest of the particles could be vesicles.

Fig. 2. Analysis of predicted viral particles from the Saint Maurice station.

The scattered signals of individual particles were resolved using the Mclust package of R software in two populations (curves: 1 red, 2 blue and in black, the sum of all curves). The number of particles, mean diameters and variances in populations 1 and 2 are noted in the inset.

Table 1: Comparison of analyzed viral particles by interferometric light (ILM) and transmission electron microscopy (TEM).

		Interferometric light microscopy[£] ILM				Transmission electron microscopy TEM		
	Particle concentrations in the water column (mL^{-1})	**Number of particles[#]**	**Number of predicted viruses (% vs. particles)**	**<60 nm (%)**	**≥60 nm (%)**	**Number of particles[*]**	**<60 nm (%)**	**≥60 nm (%)**
April 1	$5\ 10^7$	331	141 (42)	93	7	174	74	26
April 22	$8\ 10^7$	830	535 (64)	81	19	172	67	33
May 14	$3\ 10^8$	2243	1625 (72)	58	42	308	74	26

[£]The same samples were concentrated 50 or 10,000 times for ILM and TEM, respectively

#Number of particles for which we measured the diameter by scattering signal and by Brownian motion.

[*]Number of particles analyzed from about 20 TEM images.

Supplementary material for on-line submission

PCR-DGGE

Genomic DNA was extracted in duplicate from PVDF filters (Millipore) using the PowerSoil DNA isolation kit (MO BIO Laboratories, Inc). Amplification was performed with specific primers for DGGE (Table S1) to amplify fragments from 16S and 18S ribosomal DNA to study bacterial and eukaryotic diversity, respectively. Denaturing gradient gel electrophoresis (DGGE) was performed using the Phor-U system (Ingeny) as described in [1]. All PCR products were run on a single gel for the 16S and another for the 18S. After development of the DGGE polyacrylamide gel, each image was analyzed to determine similarities between profiles using the software GelCompar II 6.6 (Applied, Math). Each of the two gels was normalized based on an external reference pattern (the 100 bp ladder, Invitrogen) required by the software to compare lanes. Each band of a lane was automatically assigned to a band class, and all band classes were manually checked and eventually overridden to make them consistent between lanes. The Jaccard coefficient was calculated considering only the presence/absence of bands, each representing an operational taxonomic unit (OTU). Aquatic prokaryotic and eukaryotic communities could be compared thanks to their similarity percentages.

PCR amplification of viral fragments

We first established amplification conditions directly with known viruses of Siphovirus, Myovirus, Podoviruses and PhycoDNAvirus. Then, each concentrated filtrate (50x) from water samples was used as a template with the following program: after initial denaturation at 95°C, 1 min annealing at 50°C and 1.5 min of extension at 72°C for 35

297 cycles. PCR products were electrophoresed in 1% agarose gels in TAE buffer. Primers are
298 listed in Table S1.

299

References

[1] Roose-Amsaleg C, Yan C, Hoang AM, Laverman AM, Chronic exposure of river sediments to environmentally relevant levels of tetracycline affects bacterial communities but not denitrification rates. Ecotoxicology 2013;22:1467-1478.

[2] van Hannen EJ, van Agterveld MP, Gons HJ, Laanbroek HJ, Revealing genetic diversity of eukaryotic microorganisms in aquatic environments by denaturing gradient gel electrophoresis. J Phycol 1998;34:206-213.

[3] Muyzer G, de Waal EC, Uitterlinden AG, Profiling of complex microbial populations by denaturing gradient gel electrophoresis analysis of polymerase chain reaction-amplified genes coding for 16S rRNA. Appl Environ Microb 1993;59:695-700.

[4] Filée J, Tetart F, Suttle CA, Krisch HM, Marine T4-type bacteriophages, a ubiquitous component of the dark matter of the biosphere. P Natl Acad Sci USA 2005;102:12471-12476.

[5] Parvathi A, Zhong X, Jacquet S, Dynamics of various viral groups infecting autotrophic plankton in Lake Geneva. Adv Oceanogr Limnol 2012;3:171-191.

[6] Larsen JB, Larsen A, Bratbak G, Sandaa RA, Phylogenetic analysis of members of the *Phycodnaviridae* virus family, using amplified fragments of the major capsid protein gene. Appl Environ Microb 2008;74:3048-3057.

[7] Allen LZ, Ishoey T, Novotny MA, McLean JS, Lasken RS, Williamson SJ, Single Virus Genomics: A new tool for virus discovery. PLoS One 2011;6:1-9.

Legends to figures

Fig. S1. DGGE analysis for eukaryotic (A) and prokaryotic (B) plankton from the Marne River at St Maurice screened via their 18S and 16S rRNA gene, respectively. From the bottom to the top of the figure, processed images by Gelcompar II, resulting similarity dendrogams of Jaccard index and histogram of number of OTUs.

Fig. S2. Transmission electron microscopy analysis of Saint Maurice water samples. The pies describe viral morphotype compositions of each sample (at least 100 particles were considered).

Fig. S3. Electron micrograph of concentrated (10,000x) water sample from the Marne River (May 14th). Examples of Myovirus and Siphovirus are shown by a white or black arrow, respectively. A membrane vesicle and an untailed virus are shown by a red or green arrow, respectively. Filaments could correspond to free DNA.

338 **Table S1: List of primers used in this study**

339

Primer name	Sequences (5'-3')	Amplicon size (bp)	Target	References
F1427-GC	$(GC)_{20}$ TCT GTG ATG CCC TTA GA	229	18S ribosomal DNA	[2]
R1616	GCG GTG TGT ACA AAG GG			
F357-GC	$(GC)_{20}$ CCT AGC GGA GGC AGG AG	201	16S ribosomal DNA	[3]
R518	ATT ACC GCG GCT GCT GG			
MZPA1BF	GAT ATT TGI GGI GGT CAG CCI ATG A	550	Major capsid protein of Myoviruses	[4]
MZPA1BR	CGC GGT TGA TTT CCA GCA TGA TTT C			
Pol F	CCA AAY CTY GCM CAR GT	650-750	DNA polymerase of Podoviruses	[5]
Pol Rb	CTC GTC RTG DAT RAA SGC			
Mcp F	GGY GGY CAR CGY AAT	347-518	Major capsid protein of PhycoDNAviruses	[6]
Mcp R	TGI ARY TGY TCR AYI AGG TA			
lbdintF	TGA TAC TGT GCC GGA TGA AA	750	Integrase of Siphoviruses	[7]
lbdintR	TTA GGC AGA GAC AGG CGA AT			

340

341

Figure 1

April 1st

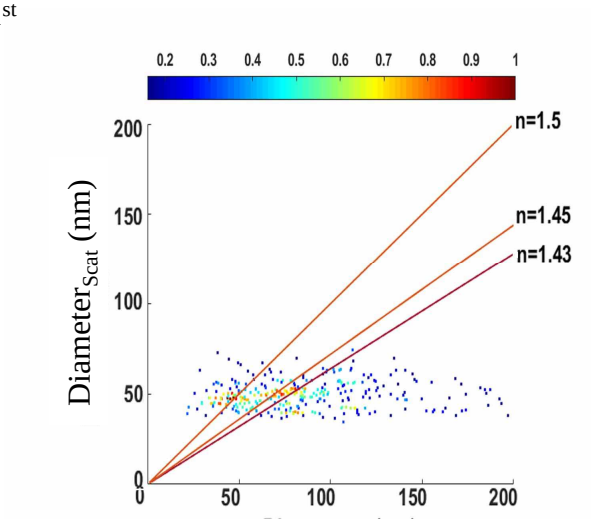

April 22th

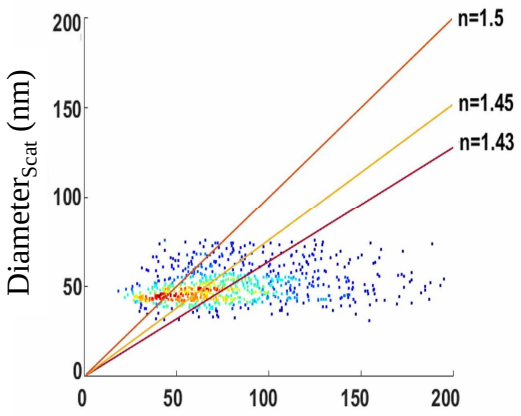

May 14th

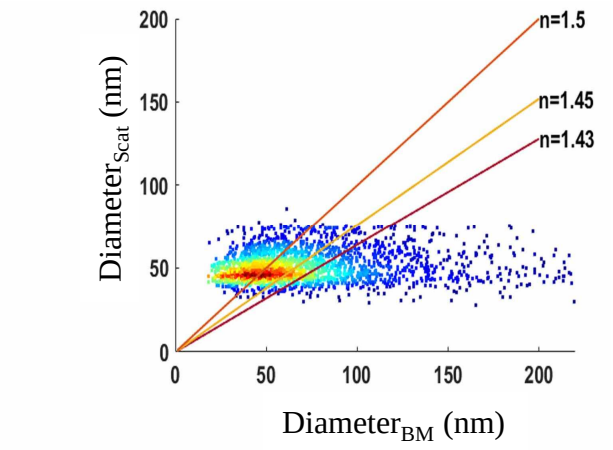

Figure 2

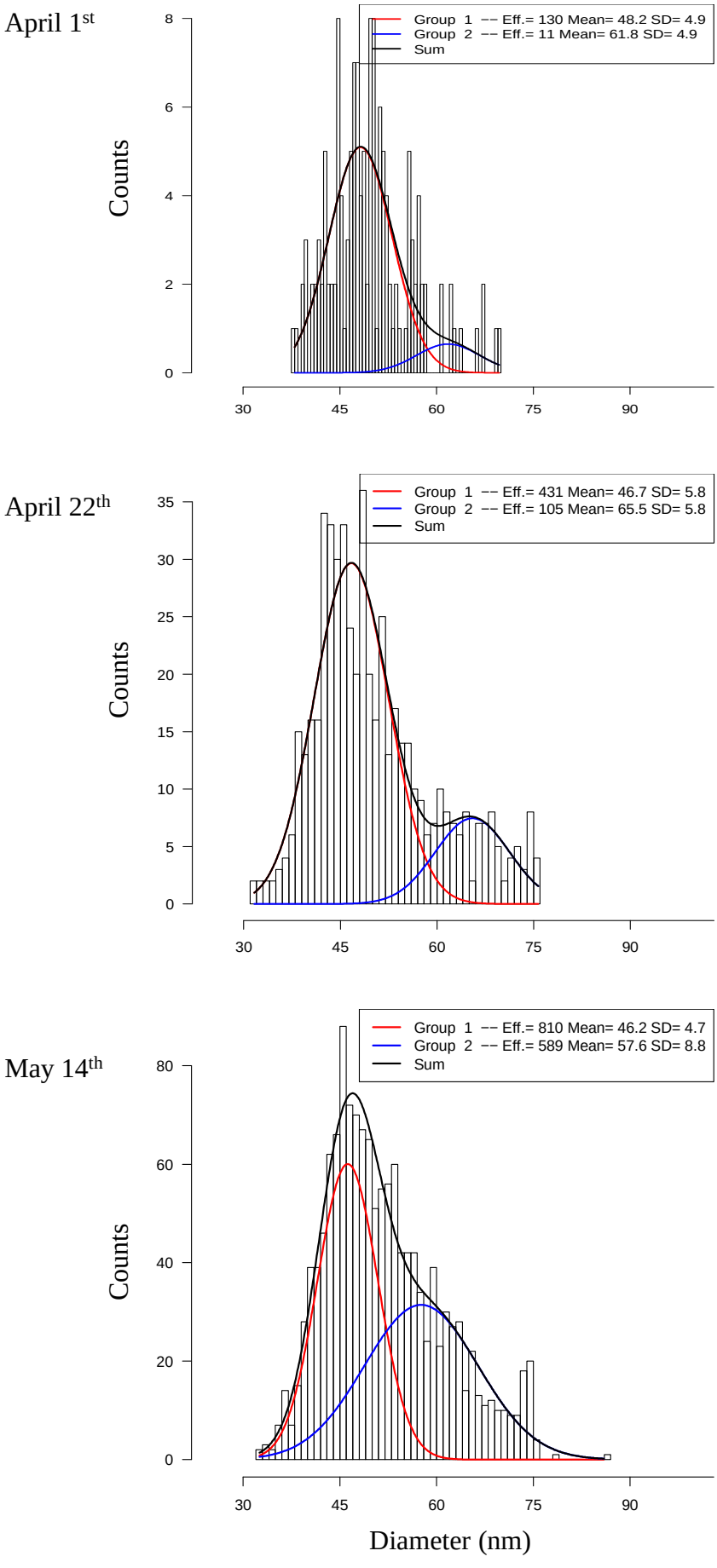
April 1st
Group 1 -- Eff.= 130 Mean= 48.2 SD= 4.9
Group 2 -- Eff.= 11 Mean= 61.8 SD= 4.9
Sum
Counts
April 22th
Group 1 -- Eff.= 431 Mean= 46.7 SD= 5.8
Group 2 -- Eff.= 105 Mean= 65.5 SD= 5.8
Sum
Counts
May 14th
Group 1 -- Eff.= 810 Mean= 46.2 SD= 4.7
Group 2 -- Eff.= 589 Mean= 57.6 SD= 8.8
Sum
Counts
Diameter (nm)